PA6–Se–Cd composite obtained via two-step assembly synthesis route

Valentina Krylova*,

Nijolė Dukštienė,

Skirma Žalenkienė

*Department of Physical and
Inorganic Chemistry,
Kaunas University of Technology,
Radvilėnų St. 19,
LT-50254 Kaunas, Lithuania*

PA6–Se–Cd composites were obtained by two-step assembly synthesis route. Firstly, a chemical bath deposition method was employed for preparation of PA6–Se precursors at room temperature using H_2SeO_3 and Na_2SO_3 solutions. These chalcogenized polymers further serve as proxies for cadmium selenide formation. The formation of CdSe is attained by exposing the PA6–Se precursor into a $Cd(CH_3COO)_2$ solution at different temperatures. The obtained composites were characterized by atomic absorption spectroscopy, optical microscopy and X-ray diffraction analysis. The Se consumption rate represents a global reaction system because it depends on the simultaneous occurrence of the heterogeneous reaction between Cd^{2+} ions and Se in the polyamide 6 (PA6) matrix and the selenium washout from polymer. The prepared PA6–Se–Cd composites are reproducible, uniform and pinhole-free. X-ray diffraction analysis showed the formation of cadmium selenide (CdSe) and selenium (Se_8) phases with a hexagonal and a monoclinic unit cell, respectively.

Keywords: selenium, cadmium selenide, polyamide 6, crystalline structure, X-ray diffraction analysis

INTRODUCTION

Polymers modified with the inorganic nanoparticles combine the functionalities of polymer matrices, which include a low weight and easy formability, with the unique features of inorganic nanoparticles. The modification of polymer with different types of inorganic materials improves its optical, mechanical, electrical, magnetic, rheological and flame retardation properties [1–2]. There is currently a great interest in II–VI semiconductor particles, particularly of cadmium selenide organically capped or embedded in polymeric matrices for their importance as light harvesting materials [3–4].

Typically, nanocomposites of polymer embedded metal chalcogenides are synthesized via in situ polymerization [5–7]. This involves the multistep organic solution processing of each element or its precursor and results in metal chalcogenides within the volume of the polymer [8]. The organic synthesis methods are generally complicated and expensive as well as the materials used are very toxic which is clearly undesirable. Therefore, it still remains a challenge to produce well dispersed metal selenide nanoparticles via an economical and simple method. The aqueous solution synthesis is

generally preferred to overcome drawbacks of organic solution methods [9]. Chemical bath deposition (CBD) can be performed at lower temperatures but it is difficult to control the shape and size of crystals or films. During chemical bath deposition, most of the materials precipitate in the powder form [10], which can be avoided in the SILAR method [11]. An interesting and promising method to deposit thick films on a polymer surface is a stepwise assembly depending on pre-constructed precursors [12]. Currently, this stepwise assembly method is far less developed than the CBD or SILAR procedure. Consequently, the possibilities offered by the combination of different step types and the ability to tailor the composition, microstructure and properties of materials are practically unexplored, and therefore open new methodological possibilities.

In the present investigation, we have tried to synthesize cadmium selenide nanocrystals into a continuous dielectric polyamide 6 (PA6) matrix through a cheap and green synthesis. The development of composites consisting of a continuous matrix with dispersed nanoparticles of II–VI semiconductor nanocrystals and studies of their optical properties are nowadays important activities in material science [3–4]. The choice of polyamide 6 as the polymer matrix was guided mainly by its properties. PA6, also known as Nylon, is widely used in variety of applications including automotive,

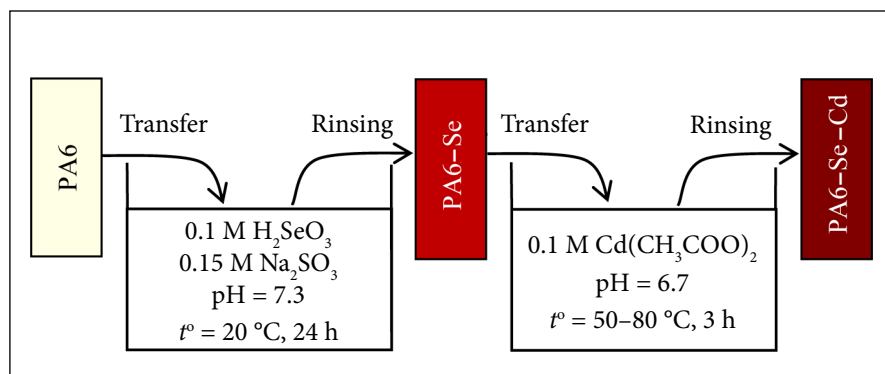* Corresponding author. E-mail: valentina.krylova@ktu.lt

Fig. 1. The principal scheme of PA6–Se–Cd composite synthesis route

textile, medicine and engineering solutions. Great mechanical properties, resistivity to abrasion and chemicals are the main properties of PA6 [13]. However, the polyamide 6 is transparent in the visible spectral range [14].

Cadmium selenide (CdSe) is an n-type semiconductor material with a band gap of 1.74 eV at 300 °K [15]. The bulk form of CdSe is not very interesting but CdSe nanoparticles are one of the most interesting semiconductors on which characteristics and applications many current researches have focused. CdSe nanoparticles exhibit size-dependent optical properties for optoelectronic devices [16], laser diodes [17], nanosensing, biomedical imaging [18–19] and high efficiency solar cells [20–21].

In our opinion, combining the unique optical properties of CdSe nanoparticles with the mechanical flexibility of PA6 gives the possibility to create a unique material for development of lightweight, flexible polymer solar cells.

The PA6–Se–Cd composites were fabricated via the two-step process (Fig. 1). Firstly, the chemical bath deposition method was employed for preparation of PA6–Se precursors at room temperature using H_2SeO_3 and Na_2SO_3 solutions. These chalcogenized polymers further served as proxies for cadmium selenide formation. The formation of CdSe was attained by exposing the PA6–Se precursor to a $Cd(CH_3COO)_2$ solution at different temperatures. We have investigated whether nanoparticles can be formed by altering the synthesis conditions of cadmium precursor exposure temperature. Finally, the morphological and structural properties of obtained composites were examined. The results herein are reported for the optimized preparative parameters that have been used to deposit good quality and reproducible PA6–Se–Cd composites. A more detailed study on the optical properties of these composites is still in progress.

EXPERIMENTAL

Materials
Distilled water was prepared in a laboratory, while chemically pure reagents were used to prepare reactive solutions. H_2SeO_3 (>99%, Reachim, Russia), Na_2SO_3, (>99%, Reachim, Russia),

and $Cd(CH_3COO)_2 \cdot 2H_2O$ (>99%, Sigma-Aldrich, Germany) were used as received. Only freshly prepared and not de-aerated solutions were used in each experiment.

Polyamide 6 films used in this study were obtained from Ensinger (Germany). The PA6 films were 500 μm thick with the density of 1.13 g · cm⁻³. Prior to the experiments, the PA6 films 15 × 70 mm in sizes were boiled in distilled water for 2 h to remove a remainder of monomer. Then they were dried using a filter paper and kept in a desiccator over $CaCl_2$ for 24 h.

Synthesis of PA6–Se–Cd composites
The chemical bath deposition technique was used to prepare the PA6–Se precursors. Prior to optimizing the bath conditions, a large number of trails for different conditions with regard to temperature, concentration of solutions and pH were performed. The concentrations of H_2SeO_3 and Na_2SO_3 solutions, and temperature that yielded the superior PA6–Se precursor, with respect to continuity, smoothness and adherence to the substrate, were chosen for further experiments.

Mixing both H_2SeO_3 and Na_2SO_3 solutions in a molar ratio of 1:2 leads to an isolation of elemental selenium according to the following reaction [22]:

$$H_2SeO_3 + 2Na_2SO_3 \rightarrow Se + 2Na_2SO_4 + H_2O. \quad (1)$$
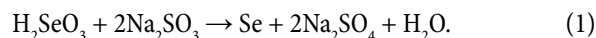
The rate of this reaction is very high. Therefore, in order to avoid the rapid formation of selenium precipitates on the bottom of the reactor, the concentration of Na_2SO_3 was chosen below the stoichiometric one.

The chemical deposition bath was prepared in a 500 cm³ beaker by the sequential addition of 200 cm³ of 0.1 M H_2SeO_3 (pH 1.42) and 200 cm³ of 0.15 M Na_2SO_3 (pH 9.43) solutions. The mixture was stirred with a glass rod to form a homogeneous solution. The pH of the working solution measured by a pH-meter WTW330 (Germany) was 7.3. The solution temperature was 20 °C. The PA6 samples were inserted vertically along the wall of the reactor and were left undisturbed for 24 h. The colourless solution with time

started to turn slowly to a yellowish colour and at the end of deposition time a red deposit formed both on the PA6 samples and on the wall of the reactor. At the end of the chosen deposition time, the samples were taken out and one sample was set aside, while the rest were cleaned with ethanol to remove a layer of poorly adherent coating and then used for the PA6–Se–Cd composite formation. The chalcogenized polymer plates were immersed in the freshly prepared $Cd(CH_3COO)_2$ solution (0.1 M, pH 6.7). In each experiment the exposure time was 3 h while the solution temperature was changed from 50 to 80 °C. The obtained PA6–Se–Cd composites were cleaned with ethanol to remove porous dendrites and then held in a desiccator over the anhydrous $CaCl_2$ for 24 h, after that subjected to characterization. The experimental conditions of the sample synthesis are summarized in Table 1.

Table 1. **Experimental conditions of the PA6–Se–Cd composite synthesis and sample labelling**

Exposure time of PA6 sample in 0.1 M H_2SeO_3/0.15 M Na_2SO_3 solution at 20 °C, h	The obtained PA6–Se samples were immersed in 0.1 M $Cd(CH_3COO)_2$ solution for 3 h at temperature of, °C	Sample labelling
24	–	PA6–Se
24	50	PA6–Se–Cd-1
24	60	PA6–Se–Cd-2
24	70	PA6–Se–Cd-3
24	80	PA6–Se–Cd-4

Characterisation techniques

Optical microscopy of the samples was carried out by an optical microscope Olympus CX31 (Olympus, Philippines) and a photocamera Olympus C-5050 (Olympus, Japan), magnification ×100.

The XRD analysis of the samples was performed on a Bruker D8 Advance diffractometer, operating at the tube voltage of 40 kV and the tube current of 40 mA. The X-ray beam was filtered with a Ni 0.02 mm filter to select the CuKα (λ = 0.154178 nm) radiation. The diffraction patterns were recorded in a Bragg–Brentano geometry using a fast counting detector Bruker LynxEye based on silicon strip technology. The specimens of the samples were scanned over the range 2θ = 2–70° at a scanning rate of 1° min^{-1} using a coupled two theta/theta scan type. The X-ray diffraction data were analysed with Search Match and Excel computer programs.

Concentrations of Se and Cd were determined using a Perkin Elmer Analyst 400 atomic absorption spectrometer (AAS). Before the analysis, the obtained samples were mineralized in hot concentrated HNO_3 to digest the PA6. In order to remove the excess of nitrogen oxides, concentrated hydrochloric acid was added to the obtained solution. Cd was determined at a wavelength of 228.80 nm and Se at a wavelength of 196.03 nm.

RESULTS AND DISCUSSIONS

Chemical analysis

Initially, the chemical composition of obtained PA6–Se–Cd composites was determined. According to the obtained results (Table 2), the value of Cd:Se molar ratio depending on the $Cd(CH_3COO)_2$ solution temperature varies from 0.55 to 0.82 and deviates from the stoichiometry showing the PA6–Se–Cd composite is selenium-rich (Table 2). Moreover, the increasing of $Cd(CH_3COO)_2$ solution temperature leads to a significant decrease of selenium amount in the PA6–Se–Cd samples as compared to that of PA6–Se (Table 2). The washout of selenium is significantly dependent on temperature that consequently alters the material stoichiometry. With changing temperature from 50 to 80 °C the selenium loss varies from 73.2 to 55.5%, respectively. In our opinion, selenium particles could be washed out from the polymer due to the thermal motion when exposing the PA6–Se precursor into the solution.

Table 2. **Bulk chemical composition of the synthesised PA6–Se–Cd composites**

Sample	Cd, mmol/g	Se, mmol/g	Molar ratio of Cd:Se
PA6–Se	–	0.508 ± 0.016	–
PA6–Se–Cd-1	0.075 ± 0.005	0.136 ± 0.004	0.55
PA6–Se–Cd-2	0.099 ± 0.003	0.133 ± 0.006	0.74
PA6–Se–Cd-3	0.139 ± 0.018	0.169 ± 0.008	0.82
PA6–Se–Cd-4	0.166 ± 0.003	0.226 ± 0.004	0.74

It seems that the Se consumption rate represents the global reaction system because it depends on the simultaneous occurrence of the heterogeneous reaction between Cd^{2+} ions and Se in the PA6 matrix and the selenium washout from polymer. Further studies are required to achieve detailed information on the kinetic aspects of heterogeneous reactions involved in the CdSe formation as well as selenium washout from the polymer process.

Optical microscopy

The PA6–Se–Cd composites were brown in colour, homogeneous, spectacularly reflecting with good adherence. The optical micrographs of the PA6–Se precursor and the corresponding PA6–Se–Cd composite are compared in Fig. 2. Fig. 2a displays a view of the PA6–Se precursor with selenium particles dispersed over the substrate. The sample shows a non-homogenous structure with a large number of micro bumps and irregularly spread dendrites. On the other hand, the homogenous distribution of selenium nanoparticles throughout the volume of PA6 polymer is clearly seen after removing the top coating from the PA6–Se surface (Fig. 2b). In contact with the PA6 surface, the electrostatic interactions between colloidal selenium particles and the charged sites of the polymer take place, providing good selenium sorption and diffusion throughout the volume of PA6 [23].
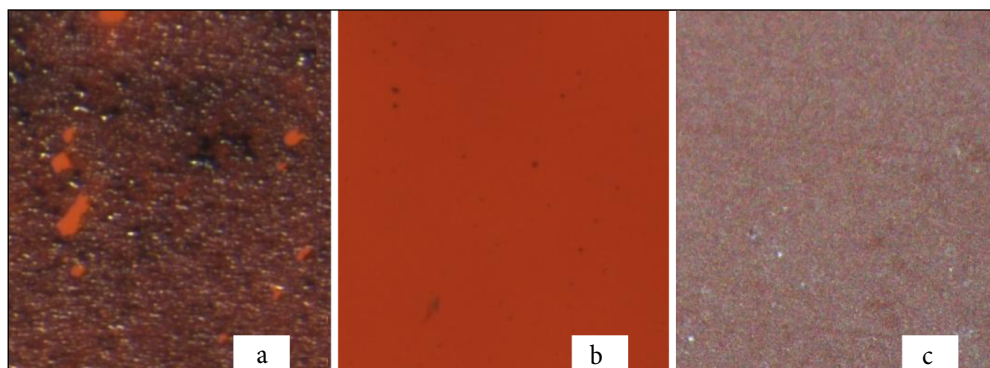
Fig. 2. Optical micrograph image of the PA6–Se precursor with top coating (a), cleaned (b) and the PA6–Se–Cd composite (c). Magnification ×100

Treatment of PA6–Se in the Cd^{2+} precursor solution leads to the formation of CdSe. The formation of CdSe results in change of the PA6–Se colour from red to brown, as shown in Fig. 2c. From optical microscopy studies, it was clarified that the surface of the PA6–Se–Cd composite is dense, without cracks and pinholes, composed of structural features similar to grains, channels and small agglomerates.

XRD analysis

To determine the structural properties of PA6–Se–Cd composite, the X-ray diffraction (XRD) patterns were analyzed. A survey of available literature shows that the CdSe can be hexagonal (wurtzite) [24], cubic (zinc-sphalerite) [25] or of a mixed structure [JCPDS files No. 19–191 and 65–2891].

At room temperature and atmospheric pressure, the major allotropic forms in which selenium exists are crystalline (trigonal, α-, β-, γ-monoclinic), amorphous (red, brown and black Se) and vitreous selenium [26]. The amorphous Se is known to have a low crystallization temperature and it transforms to crystalline forms on heating to 60–80 °C [27].

XRD diffractograms of the composites obtained at different $Cd(CH_3COO)_2$ solution temperature, while the temperature was changed from 50 to 80 °C, are presented in Fig. 3. According to the Joint Committee on Powder Diffraction Standards reference (JCPDF No. 43-1661), diffraction peaks appearing at $2\theta = 20.05°$ and $23.45°$ are attributable to the (100)α and (002/202)α crystal planes of PA6, respectively. The obtained diffraction peak positions were compared with the standard values and are mainly indexed as
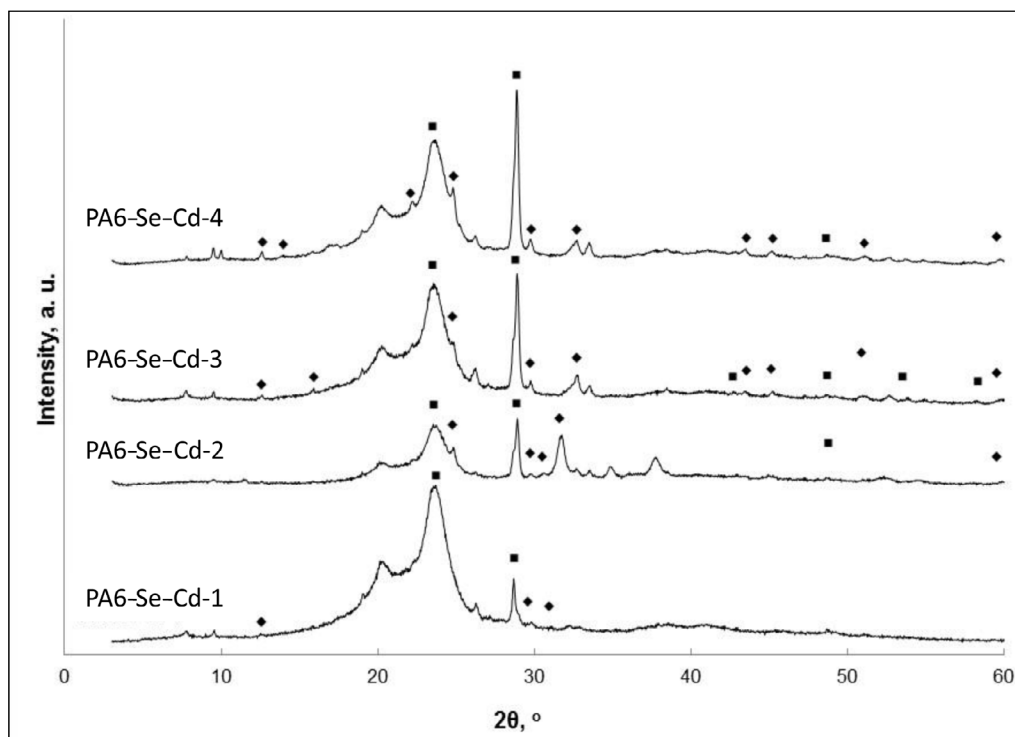

Fig. 3. XRD spectra of the PA6–Se–Cd composites, obtained at a different temperature as indicated in Table 1. ♦ is Se, ■ is CdSe

CdSe and Se_8 with a hexagonal and a monoclinic unit cell, respectively (Tables 3–6).

As shown in Fig. 3 (curves 1 and 2), the structural properties of the obtained PA6–Se–Cd composite are greatly influenced by the $Cd(CH_3COO)_2$ solution temperature.

As the deposition temperature increases, the X-ray diffraction peaks corresponding to CdSe are not shifted, indicating the same structure, regardless of the temperature used for the deposition. Figure 3 shows also that the intensities of peaks increase with the deposition temperatures, further indicating that the crystallinity of PA6–Se–Cd increased. The CdSe is found to have a polycrystalline nature with (101) being the dominant orientation plane. The present experimental result is quite consistent with reported literature data. It is well known [28] that in the case of the hexagonal lattices the strongest chemical bonds are realized by atoms placed in a semi-crystal configuration on the crystallographic planes (110) or (101).

The grain size of CdSe crystallites was calculated from XRD patterns using the Debye–Scherer's formula [29]

$$D = \frac{k\lambda}{\beta \cdot \cos\theta},$$ (2)

where λ is the X-ray wave length (0.154056 nm), and k is the shape factor and the value used in this study was 0.89. β is the full-width at half maximum (in radian), and θ is the Bragg diffraction angle.

The grain size of CdSe calculated for the (101) plane is independent of the $Cd(CH_3COO)_2$ solution temperature and is approximately 33.52 ± 1.3 nm.

As seen from Fig. 3, the preferred orientation of selenium is along the (023) plane. Moreover, the temperature of $Cd(CH_3COO)_2$ solution has a significant influence on amorphous selenium crystallization. The XRD pattern of selenium corresponding to the (023) plane showed an increase in the diffraction peak intensity and an increase in the FWHM whereas the diffractograms also displayed new peaks attributable to monoclinic selenium (Fig. 3, curves 2–4, Tables 3–6), confirming the formation of well-crystallized Se particles. The broadening of diffraction peaks is primarily due to the finite size of the crystallites. The calculated grain size values considering the (023) plane of monoclinic Se_8 vary between 31.51 and 25.70 nm and the best crystallinity is obtained at 80 °C temperature.

Table 3. **Comparison of the observed and standard "d" values of CdSe and Se in the PA6–Se–Cd-1 composite**

Temperature of $Cd(CH_3COO)_2$ solution, °C	Experimental data		Se JCPDS#71-528		CdSe JCPDS#77-2307	
	2-Theta	d, nm	d, nm	hkl	d, nm	hkl
50	12.55	0.70452	0.70884	101		
	22.29	0.39854	0.40513	120/210		
	23.54	0.37762			0.37230	100
	28.70	0.31079			0.32881	101
	29.82	0.29933	0.28714	023		
	31.10	0.28733	0.27796	130		

Table 4. **Comparison of the observed and standard "d" values of CdSe and Se in the PA6–Se–Cd-2 composite**

Temperature of $Cd(CH_3COO)_2$ solution, °C	Experimental data		Se JCPDS#71-528		CdSe JCPDS#77-2307	
	2-Theta	d, nm	d, nm	hkl	d, nm	hkl
60	22.24	0.39947		120/210		
	23.54	0.37759			0.37230	100
	24.84	0.35811	0.35757	022/–103		
	28.86	0.30895			0.32881	101
	29.77	0.29988	0.29295	023		
	30.55	0.29241	0.29441	221		
	31.71	0.28196	0.28150	–301/013		
	33.53	0.26708	0.26840	–222/–213		
	34.89	0.25697	0.25687	032		
	37.74	0.23817	0.23838	132		
	48.14	0.18887	0.18908	025		
	48.73	0.18671			0.18615	200
	59.82	0.15448	0.15484	333		

Table 5. **Comparison of the observed and standard "d" values of CdSe and Se in the PA6–Se–Cd-3 composite**

Temperature of Cd(CH₃COO)₂ solution, °C	Experimental data		Se JCPDS#71-528		CdSe JCPDS #77-2307	
	2-Theta	d, nm	d, nm	hkl	d, nm	hkl
70	12.54	0.70539	0.70884	101		
	15.86	0.55844	0.55881	111		
	22.18	0.40042	0.40513	120/210		
	23.49	0.37849			0.37230	100
	24.84	0.35813	0.35757	022/−103		
	26.21	0.33975	0.33357	−212/−122		
	28.88	0.30895			0.32881	101
	29.77	0.29990	0.29441	023		
	32.71	0.27358	0.27626	014		
	33.52	0.26711	0.26840	032		
	38.45	0.23395	0.23441	214		
	42.74	0.21141	0.21145	−233	0.21495	110
	43.50	0.20786	0.20660	025		
	45.20	0.20043	0.20087	125		
	47.298	0.19203	0.19200	−422		
	48.67	0.18693	0.18627	333	0.18615	200
	51.02	0.17886	0.17879	044/423	0.17992	201
	52.68	0.17361	0.17359	−342/−432		
	53.86	0.17009	0.17040	−512/−152	0.14560	203
	54.91	0.16707	0.16676	−521/251		
	58.27	0.15821	0.15858	441	0.15856	104
	59.83	0.15445	0.15411	−442/−217		

Table 6. **Comparison of the observed and standard "d" values of CdSe and Se in the PA6–Se–Cd-4 composite**

Temperature of Cd(CH₃COO)₂ solution, °C	Experimental data		Se JCPDS#71-528		CdSe JCPDS #77-2307	
	2-Theta	d, nm	d, nm	hkl	d, nm	hkl
80	12.57	0.70382	0.7884	101		
	13.90	0.63648	0.64120	110		
	22.18	0.40044	0.40513	120/210		
	23.52	0.37799			0.37230	100
	24.81	0.35855	0.35757	022/−103		
	26.22	0.33955	0.33357	−212/−122		
	28.85	0.30917	0.30823	221	0.32881	101
	29.76	0.29993	0.29441	023		
	32.66	0.27399	0.27626	014		
	33.49	0.26732	0.26840	032		
	37.64	0.23876	0.23838	033		
	38.46	0.23387	0.23441	214		
	42.74	0.21138			0.21495	110
	43.46	0.20804	0.20660	025		
	45.16	0.20062	0.20087	125		
	48.68	0.18691			0.18615	200
	51.09	0.17864	0.17879	044/423	0.17992	201
	52.66	0.17368	0.17359	−342/−432		
	53.77	0.17034	0.17040	−512/−152		
	54.83	0.16730	0.16676	−521/251		
	59.73	0.15468	0.15411	−442/−253		

The ratio of CdSe and crystalline Se_8 phases in the composite was estimated from the respective integrated XRD peak intensities using the following equation [30]:

$$x = \left(1 + 0.8\frac{I_A}{I_B}\right)^{-1}.$$ (3)

Here x is is the weight fraction in the sample, I_A is the intensity of the CdSe diffraction peak corresponding to the 101 plane, and I_B is the intensity of the Se_8 diffraction peak corresponding to the 023 plane.

With increasing of $Cd(CH_3COO)_2$ solution temperature from 50 to 80 °C the ratio of CdSe and Se_8 phases increases from 0.08 to 0.12, respectively.

Based on an analysis of XRD results, the conclusion can be drawn that an increase of $Cd(CH_3COO)_2$ solution temperature favours the crystallization of amorphous selenium.

CONCLUSIONS

1. The PA6–Se–Cd composites were successfully obtained at 50–80 °C temperature from a cadmium acetate solution with the previous pre-treatment of polyamide 6 in a mixture of selenite acid and sodium sulphite solutions at room temperature.

2. The value of Cd:Se molar ratio in the obtained composites depending on $Cd(CH_3COO)_2$ solution temperature varies from 0.55 to 0.82.

3. The surface of the PA6–Se–Cd composite is heterogeneous composed of structural features similar to grains, channels and small agglomerates.

4. XRD analysis confirmed a formation of CdSe and Se_8 with a hexagonal and a monoclinic unit cell, respectively.

References

1. J. M. Breiner, J. E. Mark, *Polymer*, **39**, 5483 (1998).

2. M. Z. Rong, M. Q. Zhang, Y. X. Zheng, H. M. Zeng, K. Friedrich, *Polymer*, **42**, 3301 (2001).

3. S. Žalenkienė, V. Krylova, J. Baltrusaitis, *Appl. Surf. Sci.*, **325**, 175 (2015).

4. V. Krylova, A. Milbrat, A. Embrechts, J. Baltrusaitis, *Appl. Surf. Sci.*, **301**, 134 (2014).

5. X. D. Ma, X. F. Qian, J. Yin, Z. K. Zhu, *J. Mater.Chem.*, **12**, 663 (2002).

6. C. Guan, C. L. Lu, Y. R. Cheng, S. Y. Song, B. A. Yang, *J. Mater. Chem.*, **19**, 617 (2009).

7. Y. Cheng, C. Lu, Z. Lin, et al., *J. Mater. Chem.*, **18**, 4062 (2008).

8. S. Mohan, O. S. Oluwafemi, S. P. Songca, et al., *New J. Chem.*, **38**, 155 (2014).

9. L. Saravanan, S. Diwakar, R. M. Kumar, A. Pandurangan, R. Jayavel, *Nanomater. Nanotechnol.*, **1**, 42 (2011).

10. A. Mukherjee, B. Satpati, S. R. Bhattacharyya, R. Ghosh, P. Mitra, *Physica E*, **65**, 51 (2015).

11. B. Güzeldir, M. Sağlam, A. Ateş, *J. Optoelectron. Adven. Mater.*, **14(3–4)**, 224 (2012).

12. V. Krylova, S. Žalenkienė, N. Dukstienė, J. Baltrusaitis, *Appl. Surf. Sci.*, **351**, 203 (2015).

13. A. Aulova, I. Emri, *Materials Today: Proceedings of 32nd Symposium on Advanced in Experimental Mechanics,* Stary Smokovec (2016).

14. V. Krylova, J. Baltrusaitis, *Appl. Surf. Sci.*, **282**, 552 (2013).

15. S. Velumani, X. Mathew, P. J. Sebastian, S. K. Narayandass, D. Mangalaraj, *Sol. Energy Mater. Sol. Cells*, **76**, 347 (2003).

16. K. Girija. S. Thitumalairajan, S. M. Mohan, J. Chandrasekaran, *Chalcogenide Lett.* **6(8)**, 351 (2009).

17. V. T. Patil, Y. R. Toda, V. P. Joshi, D. A. Tayde, J. V. Dhanvij, D. N. Gujarathi, *Chalcogenide Lett.*, **10(7)**, 239 (2013).

18. G. Nedelcu, *Dig. J. Nanomater. Bios.*, **3(3)**, 103 (2008).

19. Gh. R. Amiri, M. H. Yousefi, M. R. Aboulhassani, et al., *Dig. J. Nanomater. Bios.*, **5(3)**, 1025 (2010).

20. S. M. Pawar, A. V. Moholkar, C. H. Bhosale. *Mater. Lett.*, **61**, 1034 (2007).

21. P. P. Hankare, S. D. Delekar, M. R. Asabe, et al., *J. Phys. Chem. Solid.*, **67**, 2506 (2006).

22. J. Sukyte, A. Ivanauskas, I. Ancutiene, *Chalcogenide Lett.*, **12(11)**, 569 (2015).

23. M. H. Kunita, E. M. Girotto, E. Radovanovic, et al., *Appl. Surf. Sci.*, **202**, 223 (2002).

24. N. A. Okereke, A. J. Ekpunobi, *Chalcogenide Lett.*, **8(6)**, 377 (2011).

25. D. K. Dwivedi, V. Kumar, M. Dubey, H. P. Pathak, *World J. Scien. Techn.*, **1**, 21 (2011).

26. V. S. Minaev, S. P. Timoshenkov, V. V. Kalugin, *J. Optoelectron. Adv. Mater.*, **7**, 1717 (2005).

27. W. Charles Cooper, R. A. Westbury, in: A. Ralph, W. Zingaro and W. Charles Cooper (eds.), *Selenium*, P. 835, Van Nostr and Reinhold Company, New York (1974).

28. S. Mahieu, P. Ghekiere, D. Depla, R. de Gryse, *Thin Solid Films*, **515**, 1229 (2006).

29. G. M. Lohar, S. K. Shinde, M. C. Rath, V. J. Fulari, *Mater. Scien. Semicond. Process.*, **26**, 548 (2014).

30. R. A. Spurr, H. Mayers, *Quantitative Analysis of Elements. X-ray Diffraction*, 2nd edn., Addison-Wesley, Reading (1978).

Valentina Krylova, Nijolė Dukštienė, Skirma Žalenkienė

**PA6-Se-Cd KOMPOZITAI, GAUTI DVIEJŲ ETAPŲ
SINTEZĖS BŪDU**

S a n t r a u k a

PA6-Se-Cd kompozitai susintetinti dviem etapais. Iš pradžių kambario temperatūroje iš vandeninių selenitinės rūgšties ir natrio sulfito tirpalų mišinio į poliamidą 6 įterptas selenas. Po to gautas PA6-Se pirmtakas transformuotas į CdSe naudojant 50–80 °C temperatūros kadmio acetato vandeninius tirpalus. Gauti PA6-Se-Cd kompozitai tirti optinės mikroskopijos, atominės absorbcinės spektroskopijos ir rentgeno struktūrinės fazinės analizės metodais. PA6-Se-Cd kompozitų susidarymą lemia dvi tuo pačiu metu vykstančios reakcijos: viena jų yra Cd^{2+} jonų sąveika su PA6-Se pirmtaku, o antroji – seleno išsiplovimas iš polimero. Rentgeno struktūrinė fazinė analizė parodė, kad PA6 matricoje įsiterpę heksagonalinis CdSe ir monoklininis Se_8.